Mine Water Environ (2017) 36:255–263
DOI 10.1007/s10230-016-0406-4

TECHNICAL ARTICLE

Removal of Dissolved Arsenic by Pyrite Ash Waste

T. Turk[1]

Received: 22 July 2015 / Accepted: 11 June 2016 / Published online: 22 June 2016

Abstract Pyrite ash (PA), a waste produced during the roasting of pyrite ores to produce sulfuric acid, was studied as a potential adsorbent for removing arsenic (As) from groundwater. The collected pyrite ash waste samples contained >86 % iron (as Fe_2O_3). The results indicate that adsorption of As by PA was only slightly affected by initial pH at pH $\leq$ 9. Arsenate removal efficiency increased with the amount of adsorbent added over the range of 0.1–50 g/L. The As(V) removal increased with time, and 79 % removal was achieved within 1 h. Moreover, there was no significant change in As concentrations after 24 h. The adsorption process was best described by a second-order kinetic model. The adsorption of As(V) onto the PA was found to have followed the Langmuir isotherm. In batch studies, the maximum As(V) removal efficiency was 97 % at an adsorbent dose of 10 g/L, with an initial As(V) concentration of 300 µg/L. Thus, the PA was shown to be a suitable sorbent, reducing As from an initial level of 600 to <10 µg/L As(V), i.e., below the WHO limit for drinking water.

Keywords Arsenate · Adsorption · Borated water · Kinetics · Isotherm

Introduction

Arsenic (As) can be released into the environment by activities such as mining and ore processing (Clara and Magalhães 2002). Arsenic can exist in the −3, 0, +3, and +5 oxidation states (Smedley et al. 2002). Pentavalent species (As(V) or arsenate) are stable in oxygen-rich aerobic environments, while trivalent (As(III) or arsenite) predominates in moderately reducing anaerobic environments (Mohan and Pittman 2007). The As oxidation state affects its toxicity, and arsenite, or As(III), is more toxic than arsenate As(V) and most organic arsenic compounds (Jomova et al. 2011; WHO 1981).

High As concentrations have been found in water sources in many countries, including the USA, China, Bangladesh, Taiwan, Mexico, Canada, Hungary, Japan, Pakistan, and India (Mukherjee et al. 2006). Natural As pollution has also been reported in Turkey within the last 10 years (Aksoy et al. 2009; Colak et al. 2003). In Turkey, especially in western Turkey, As concentrations ranging from 20 to 3000 µg/L have been encountered in groundwater resources (Başkan et al. 2010). Because of its high toxicity, the World Health Organization (WHO) lowered the maximum contaminant level for As in drinking water from 50 to 10 µg/L (WHO 1996).

The most effective As treatment processes include adsorption, ion exchange, reverse osmosis, and nanofiltration (Mondal et al. 2006). Successful As adsorption technologies include granular activated alumina, synthetic zeolites (Xu et al. 2002), granular ferric hydroxide (Arienzo et al. 2002), granular activated carbon (Chuang et al. 2005), and granular activated carbon impregnated by ferrous oxide (Vaughan and Reed 2005).

Crystalline iron oxide minerals have also been investigated for use as adsorbents for As. Hematite and goethite were reported to be effective for As removal from polluted water (Lenoble et al. 2002; Zhang et al. 2004). Natural hematite was used as adsorbent in experimental studies, and a residual As concentration below 0.05 mg/L was achieved (Zhang et al. 2004). However, most of the existing options are not cost effective for small

✉ T. Turk
tugbaturk@yahoo.com.tr

[1] Department of Mining Engineering, Karadeniz Technical University, 61080 Trabzon, Turkey

communities that depend on water supplies in which the contaminant level exceeds 10 μg/L (Makris et al. 2006). For these reasons, the potential use of waste by-products generated from different industrial processes, such as fly ash (Balsamo et al. 2010) and red mud (Altundoğan et al. 2000), have been investigated.

The Emet-Hisarcık (Turkey) region contains one of the world's largest boron (B) reserves. Unlike other areas with B mineralization, it also contains As minerals (orpiment and realgar); the groundwater associated with these deposits was reported to contain up to 600 μg/L of As and 3900 μg/L of B (Aydın et al. 2003). Therefore, As removal is required for mine water in this area.

Pyrite ash (PA) is a waste produced during the roasting of pyrite ores in sulfuric acid production. At the Eti Mine Works in Bandırma, Turkey, where PA is produced, it is generally landfilled or dumped into the sea, and is thus a potential pollution source (Tugrul et al. 2007). Alp et al. (2009) demonstrated that PA can be used as an iron source in cement production. Another possible application is to use it to remove As from the mine water. Although As is strongly adsorbed onto Fe oxides and hydroxides (Ravenscroft et al. 2009), which are abundant in PA, and adsorption can be an attractive technology if the adsorbent is cheap and ready for use (Zhang et al. 2008), there were no previous studies on As removal using PA. The present study tested this possible beneficial use of this waste material.

Materials and Methods

Pyrite Ash Waste

The PA waste samples used in this study were taken from the Bandırma Borax and Boric Acid Establishment, Balıkesir, Turkey. A whole rock analysis for the major oxides and minor elements of the pyrite ash was carried out using ICP-OES (ACME Analytical Lab), following a lithium borate fusion and dilute acid digestion of a sample pulp (Table 1). The analysis package included loss on ignition (LOI) by sintering at 1000 °C. Chemical analysis quality control was performed by analyzing STD SO-18.

The crystalline phase composition of the material was investigated using x-ray diffraction (XRD) (RIGAKU, D/Max-IIIC). The Brunauer–Emmett–Teller (BET) method was used to determine the surface area of the PA sample. The particle size distribution of the sample was determined using laser diffraction (Malvern Master Sizer).

Adsorption Tests

An arsenate stock solution was prepared by dissolving $Na_2HAsO_4{\cdot}7H_2O$ in water to a concentration of 1 g/L As(V). Fresh stock solutions of 100 mg/L As(V) were prepared every week, and these stock solutions were used to prepare the initial As(V) concentrations. Sample pH was adjusted by the addition of hydrochloric acid (1 M HCl) or sodium hydroxide (1 M NaOH) standard solutions. The flasks containing the mixtures were immersed into a 25 °C water bath and then agitated at 200 rpm with a mechanical shaker. The effects of the solution pH (3, 5, 7, and 9), adsorbent dosage (0.1, 1, 5, 10, 20, and 50 g/L), initial metal ion concentration (10, 50, 100, 300, and 500 μg/L), and contact time on As(V) adsorption were studied. The adsorption isotherms and kinetics were obtained by the batch equilibration technique. For the equilibrium studies, a series of 100 mL flasks were prepared using a 50 mL solution of As(V) (10–500 μg/L) at a fixed adsorbent concentration (10 g/L). For the kinetics studies, a series of 100 mL flasks were prepared using a 50 mL solution of As(V) (300 μg/L), at a fixed adsorbent concentration (10 g/L) and reacted over contact times of 1, 3, 5, 7, and 24 h.

Field water samples, taken from different parts of Emet-Hisarcik (Turkey), were stored in plastic containers. These samples were analyzed by Dionex IC100 ion chromatography (F^-, Cl^-, NO_3^-, NO_2^-, PO_4^{3-}, SO_4^{2-}) and Spectro Genesis ICP-OES (Mg, Ca, Si, Fe, Al, As, B). The As(V) adsorption tests were performed under initial As(V) concentrations of 600 μg/L, an initial pH of 9, various PA dosages (150, 70, 50, 20, 10, and 5 g/L) and a contact time of 5 h. At the end of the contact period, the mixture was centrifuged for 10 min at 4000 rpm, and the final pH of the supernatants was measured. The supernatants were analyzed for As(V) using a continuous hydride generation unit on an inductively coupled plasma optical emission (ICP-OES) spectrophotometer.

Table 1 Chemical composition of the pyrite ash waste

Component	%
SiO_2	8.13
Al_2O_3	1.63
Fe_2O_3	86.54
MgO	0.44
CaO	0.59
Na_2O	0.09
K_2O	0.13
TiO_2	0.13
P_2O_5	0.04
MnO	0.02
Cr_2O_3	<0.01
Ba	<0.01
Ni	<0.01
LOI	0.70
TOT/C	<0.02
TOT/S	0.49

The pzc (point of zero charge) value of the PA was determined by equilibrating the PA with 0.1 M NaCl solutions at different pH values (3–12). Details of the procedure can be found elsewhere (Pecenyuk 1999).

Results and Discussion

Adsorption of As(V) by PA

The pyrite ash sample contained significant concentrations of iron (86.54 % as Fe_2O_3) and silicon (8.13 % as SiO_2); the other metal oxides totalled less than 10 % (Table 1). The XRD analyses of the PA showed the presence of mainly hematite (Fe_2O_3) and magnetite (Fe_3O_4), a minor amount of pyrite (FeS_2), and traces of quartz (SiO_2). The particle size of 80 % of the sample and specific surface areas were found to be finer than 50 μm and 2.16 m^2/g, respectively.

The point of zero charge (pzc) is a very important value for adsorption measurements and surface characterization; in this study, it is defined as the pH at which the the electrical charge density on the surface of the particles is zero. The pzc can control sorption of protons and hydroxyl groups, which depends on the acid–base properties of the surface (Pecenyuk 1999). Previous studies reported that the pzc for the PA components were 7.9, 5.4, 6.4, and 2.1, respectively, for magnetite (Tombacz et al. 2006), hematite (Huang et al. 2001), pyrite (Borah and Senapati 2006), and quartz (Kroutil et al. 2015). In this study, the pzc values of the PA were determined to be 4.6. It should also be noted that preparation methods can influence pzc and that similar materials can have variable pzc values.

For As(V), the corresponding stable species and pH values are H_3AsO_4 (pH 0–2), $H_2AsO_4^-$ (pH 2–7), $HAsO_4^{2-}$ (pH 7–12) and AsO_4^{3-} (pH 12–14) (Türk et al. 2009). For example, when the pH is 3-9, the negatively charged $H_2AsO_4^-$ and $HAsO_4^{2-}$ are predominant.

Figure 1 shows the effects of the initial pH on the efficiency of As(V) adsorption by PA with an initial As concentration of 300 μg/L. The As adsorption was only weakly dependent on the initial pH at pH $\leq$ 9. After an adsorption period of 5 h, the residual dissolved As was 6.8 μg/L at pH 9. The PA surface was positively charged when the pH $<$ pzc 4.6. Although the adsorbent surface and the sorbate species were both negatively charged, adsorption did not decrease at pH $>$ pzc. The addition of PA was found to have a buffering effect; the final pH in the tests were 4.6–5.0 at initial pHs of 3–9. Other researchers have also observed the amphoteric effects of iron-based compounds, and Zhang et al. (2004) reported a similar buffering effect for iron ore containing hematite and goethite during adsorptive removal of As. In this study, As adsorption on PA was observed to be maximized at pH 9 (Fig. 1). The pH was kept constant at pH 9 in the adsorption tests because of the alkaline nature of the field sample solutions used in this study.

The effect of PA dosages (50, 20, 10, 5, 1, and 0.1 g/L) on adsorption of As(V) in 300 μg/L solutions is shown in Fig. 2. As(V) removal increased with the amount of PA over the range of 0.1-50 g/L, due to the additional available adsorbent surface (Genc et al. 2003). An adsorbent dosage of 10 g/L was required to reduce As concentrations down to the desired levels of <10 μg/L (Fig. 2). After a contact time of 5 h, the residual dissolved As(V) was 106.8 μg/L at a PA dosage of 0.1 g/L, compared with 8.5 μg/L at 10 g/L PA. In subsequent studies, the adsorbent dosage was set at 10 g/L.

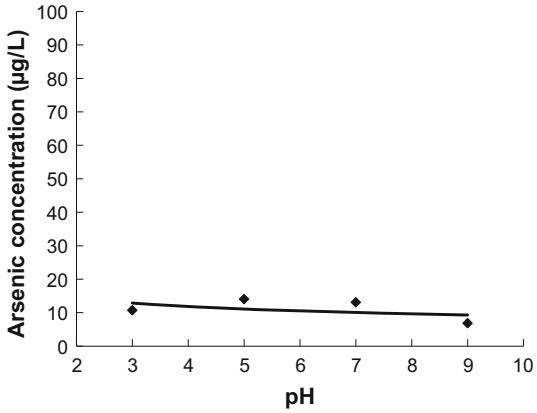

Fig. 1 Effect of final pH of mixtures on the adsorption of As(V) by PA (initial concentration: 300 μg/L; contact time: 5 h, PA dosage: 10 g/L; temperature: 25 °C)

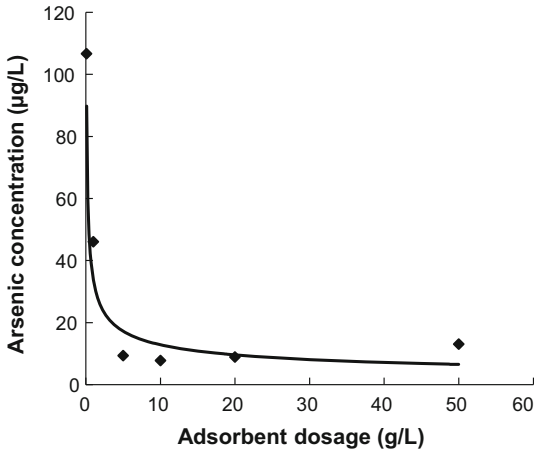

Fig. 2 Effect of PA dosage on the As(V) adsorption (initial concentration: 300 μg/L; contact time: 5 h; pH: 9; temperature: 25 °C)

Kinetic Modeling

The kinetics of the adsorption describing the rate of As removal is one of the important characteristics that define adsorption efficiency (Salim and Munekage 2009). Adsorption kinetics was used to explain the adsorption characteristics and mechanism. Two kinetics models were used: pseudo-first order and pseudo-second order. The data shown in Fig. 3 were used for analysis by taking the linear form of the following kinetic model equations:

The pseudo-first-order equation (Ho and McKay 1998) is:

$$\frac{dq_t}{dt} = k_1(q_e - q_t) \quad (1)$$

where qe and qt are the adsorption capacity (μg/g) at equilibrium and at time t respectively, and k_1 is the pseudo-first-order rate constant (min^{-1}). The linearized form of Eqs. (1) is (2).

$$\ln(q_e - q_t) = \ln q_e - k_1 t \quad (2)$$

The pseudo-second-order equation (Ho and McKay 1998) is:

$$\frac{dq_t}{dt} = k_2(q_e - q_t)^2 \quad (3)$$

The linearized form of Eqs. (3) is (4):

$$\frac{t}{q_t} = \frac{1}{k_2 q_e^2} + \frac{t}{q_e} \quad (4)$$

where both qe and qt have the same meaning as above and k_2 is the pseudo-second-order rate constant (g mg^{-1} $time^{-1}$).

The removal of As(V) increased with time; 79 % removal was achieved within 1 h (Fig. 3). There was no significant concentration change after 24 h. The slope and intercept of the plot of log ($qe - qt$) versus t were used to determine the first-order rate constant k_1 and the equilibrium adsorption density qe at the initial concentrations of As(V). The k_1 and R^2 correlation coefficients were 0.13 and 0.9270, respectively. The kinetic parameters for the pseudo-second-order model were determined from the linear plot of t/qt against t (Fig. 3). The values of k_2 and R^2 for the pseudo-second-order rate model were 0.13 g/μgh and 0.9998, respectively. The high correlation coefficients suggested that the adsorption kinetics of As(V) on PA was best described by the pseudo-second order model, indicating chemisorption (Bulut et al. 2008).

Adsorption Isotherms

Adsorption isotherm studies are important in determining the adsorption capacity of As(V) onto PA and to describe the nature of adsorption. Several isotherm equations are available, and three isotherms (Zazouli et al. 2013) were tested in this study: the Langmuir, Freundlich and Dubinin–Radushkevich (D–R) isotherms. The adsorption isotherm for As(V) removed by PA is shown in Fig. 4.

The Freundlich isotherm model has been used to describe both adsorption on heterogeneous surfaces and multilayer sorption (Foo and Hameed 2010). A higher K_f value indicates greater adsorbate removal (Raji and Anirudran 1998). The Freundlich empirical equation, Eq. (5), and its linearized form, Eq. (6), are expressed as:

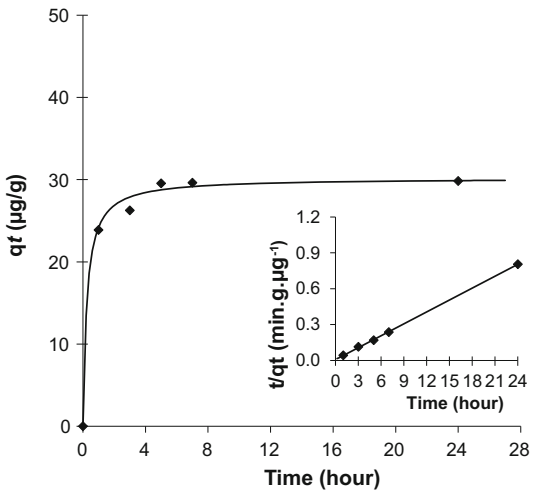

Fig. 3 Effect of contact time on the adsorption of As(V) by PA (initial concentration: 300 μg/L; pH: 9; PA dosage: 10 g/L; temperature: 25 °C). Lower inset shows pseudo-second-order plot of As(V) adsorption on PA

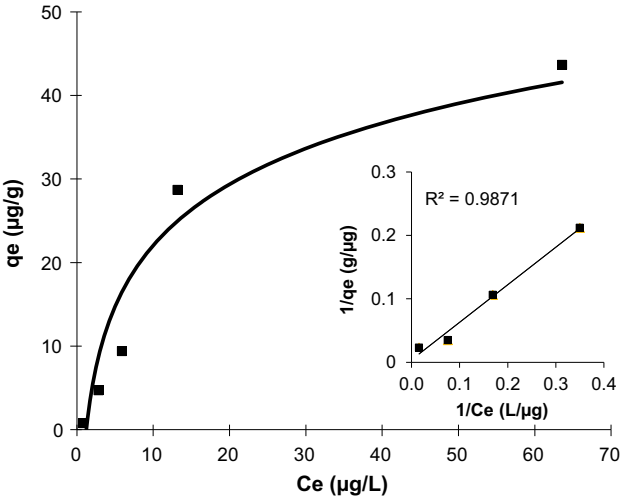

Fig. 4 Equilibrium isotherm for As(V) adsorption by PA (initial concentration: 50–500 μg/L; contact time: 5 h; pH: 9; PA dosage: 10 g/L, temperature: 25 °C) and Langmuir adsorption isotherm models for As(V) adsorption

$$q_e = K_f C_e^{1/n} \quad (5)$$

$$\ln q_e = \ln K_f + \frac{1}{n} \ln C_e \quad (6)$$

where C_e is the equilibrium concentration (μg/L), q_e the amount adsorbed under equilibrium (μg/g), and K_f and n are the Freundlich isotherm constants representing the adsorption capacity and intensity, respectively. n is a measure of deviation from linearity of the adsorption and indicates the degree of non-linearity between the solution concentration and adsorption. The linear plot of log q_e and log C_e gives a slope of $1/n$ and the intercept of log K_f. The Freundlich adsorption isotherm is also presented in Fig. 5. The Freundlich parameters Kf and n were determined to be 2.64 and 1.35, respectively ($R^2 = 0.89$).

The Langmuir isotherm describes monolayer adsorption on a uniform surface with a finite number of adsorption sites. Once a site is filled, no further sorption can take place at that site. When all the adsorption sites on the surface are saturated, maximum adsorption is achieved (Foo and Hameed 2010). The Langmuir isotherm can be determined using the following equation:

$$q_e = \frac{QbC_e}{1 + bC_e} \quad (7)$$

Equation (7) can be written in linear form using the following equation (Dada et al. 2012):

$$\frac{1}{q_e} = \frac{1}{bQC_e} + \frac{1}{Q} \quad (8)$$

where q_e is the amount of adsorbed metal per unit PA at equilibrium, Q is the saturated monolayer adsorption capacity, b is the binding energy of the sorption system, and C_e is the equilibrium concentration of the solution. The linear plots of 1/qe versus 1/Ce were obtained with a high correlation coefficient ($R^2 = 0.98$), indicating that adsorption of As(V) onto PA was consistent with the Langmuir isotherm model (Fig. 4).

The D–R isotherm model is used to distinguish between physisorption and chemisorption and to assess the adsorption mechanism. The D–R isotherm model is related to the porosity of the adsorbent. It assumes that adsorption is multilayered and involves van der Waals forces. Additionally, this model is applicable for physical adsorption (Dubinin 1960). The D–R adsorption isotherm can be expressed as:

$$q_e = Q_D \exp\left(-B_D \varepsilon^2\right) \quad (9)$$

and linearized as:

$$\ln q_e = \ln Q_D - B_D \varepsilon^2 \quad (10)$$

where Q_D is the theoretical maximum capacity (mol/g), B_D is the D–R model constant (mol^2/kJ^2), and ε is the Polanyi potential, equal to $\varepsilon = RT \ln\left(1 + \frac{1}{C_e}\right)$

Figure 5 shows the plot of ln qe against ε^2, which was almost linear with a correlation coefficient of $R^2 = 0.82$. Q_D and B_D were calculated from the slope and intercept of the plot, respectively. B_D was found to be 3.64 mol^2/(J^2), and Q_D was 30.09 mol/g.

The mean free energy of adsorption (E) was calculated using $E = \frac{1}{\sqrt{2B_D}}$(Hobson 1969). The value of E is very useful in predicting the type of adsorption. If E is less than 8 kJ/mol, the adsorption is physical, and if it is between 8 and 16 kJ/mol, the adsorption is chemisorption (Islam et al. 2011). The value of E was 0.26 kJ/mol (Table 2), indicating physical adsorption.

As shown in Figs. 4 and 5 and Table 2, according to the correlation coefficients (R^2), a suitability order of the three models tested was Langmuir, Freundlich, and D–R (Table 3), which indicates that the Langmuir model best describes the As(V) adsorption isotherm for PA. This may be because the Langmuir model assumes that the pyrite ash surface is homogeneous (Foo and Hameed 2010). Gimenez et al. (2007) also studied the sorption of As(V) on natural hematite, magnetite, and goethite and found it to be consistent with the Langmuir model. The essential

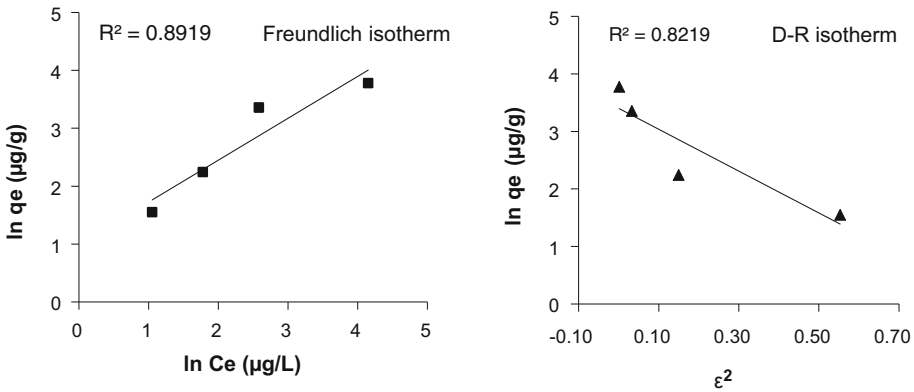

Fig. 5 Freundlich and D–R adsorption plots for As(V) adsorption on PA

Table 2 Calculated Langmuir and Freundlich isotherm parameters for As(V) adsorption on PA (pH: 9; PA dosage: 10 g/L; temperature: 25 °C)

Parameter	Value	R^2
Langmuir isotherm		
Q (μg/g)	294.6	0.98
b	0.005	
Freundlich isotherm		
K_f	2.64	0.89
n	1.35	
D–R		
Q_D	30.09	0.82
B_D	3.64	

characteristics of the Langmuir isotherm model can be explained in terms of a dimensionless constant separation factor or equilibrium parameter R_L (Kundu and Gupta 2007), which is defined by Eq. (11)

$$R_L = \frac{1}{1 + bC_o} \tag{11}$$

where b is the Langmuir constant (L/μg) and C_o is the initial concentration (μg/L). The values of R_L for our experiments were found to be less than 0.4. Since $R_L < 1$ represents positive adsorption (Kundu and Gupta 2007), adsorption of As(V) by PA is favored.

The Langmuir isotherm data also show that the adsorbed As ions formed a monolayer and do not interact or compete with each other. This also indicates that chemisorption is the principal uptake mechanism (Zhou et al. 2009). The isotherm study was studied using different initial As concentrations ranging from 10 to 300 μg/L at 25 °C, a pH of 9, and a PA dosage of 10 g/L after 5 h. The maximum adsorption capacity was found to be 294 μg/g of As using the Langmuir isotherm, which is comparable to the adsorption capacities of other As adsorbents (Table 4). Siderite (30 % Fe) had a lower adsorption capacity than hematite (56.5 % Fe), nanomagnetite (64.1 % Fe), and pyrite ash (60.5 % Fe), while natural iron ore (66 % Fe) had a higher adsorption capacity (400 μg/g).

Singh et al. (1996) used a suspension containing a known amount of hematite to study As removal in an aqueous solution. In their study, the maximum adsorption capacity of hematite was 219 μg/g for an initial As concentration of 10,000 μg/L. Türk et al. (2010) focused on As removal with nanomagnetite. The equilibrium capacity of NM was determined to be ≈204 μg/g at an initial As(V) concentrations of 100–2000 μg/L at pH 9.

Examination of Groundwater

The As and B content of the water samples taken from different parts of Emet are summarized in Table 5. The As levels makes water treatment necessary prior to use. The boric acid and enriched plant wastewater had very high As concentrations (Table 5), which can best be removed by methods such as precipitation or coagulation (Başkan et al. 2010). Song et al. (2006) reported that enhanced coagulation, followed by conventional filtration, achieved very high As removal (99 %) from high-arsenic water (5 mg/L of As). Because adsorption is generally preferred for less polluted (100–500 μg/L) and drinking water treatment (Torrens 1999), drinking water well 3, which contained lower As concentrations, was selected as representing a natural solution.

This natural solution still had relatively high As (613 μg/L) and B (3936 μg/L) concentrations; the As concentrations significantly exceeded the WHO (1993) and TS 266 (2005) drinking water standards (<10 μg/L). The natural water elemental concentrations (Table 6) were measured by Dionex IC100 ion chromatography (F^-, Cl^-, NO_3^-, NO_2^-, PO_4^{3-},SO_4^{2-}) and Spectro Genesis ICP-

Table 3 List of adsorption isotherms models

Isotherm	Nonlinear form	Linear form	Plot	References
Langmuir	$q_e = \frac{QbC_e}{1+bC_e}$	$\frac{1}{q_e} = \frac{1}{bQC_e} + \frac{1}{Q}$	1/*q*e versus 1/C_e	Kundu and Gupta (2007)
Freundlich	$q_e = K_f C_e^{1/n}$	$\ln q_e = \ln K_f + \frac{1}{n} \ln C_e$	ln q_e versus ln C_e	Veli and Akyüz (2007)
Dubinin–Radushkevich (D–R)	$q_e = Q_D \exp(-B_D\varepsilon^2)$	ln q_e = ln Q_D - $B_D\varepsilon^2$	In q_e versus ε^2	Dubinin (1960)

Table 4 Comparison of arsenic adsorption capacity of pyrite ash with some reported adsorbents, using the Langmuir isotherm model

Adsorbent	Initial Conc. (μg/L)	Surface area (m^2/g)	*Q* (μg/g)	References
Hematite	10,000	14.4	219	Singh et al. (1996)
Natural iron ores	1000	10.2	400	Zang et al. (2004)
Siderite	1000	8.5	98	Guo et al. 2007
Nanomagnetite	500	60	371	Cong 2004
Pyrite ash	500	2.16	294.6	Present work

Table 5 As and B content of the water samples

Sample definition	As (μg/L)	B (μg/L)
well-1	82	770
well-2	138	3876
well-3	613	3936
Enrichment plant wastewater	4233	2115
Boric acid plant wastewater	454,076	7926

Table 6 Chemical analysis of the natural water sample (well-3)

Component	F^-	Cl^-	NO_2^-	NO_3^-	PO_4^{-3}	SO_4^{-2}	
(mg/L)	0.7	6.85	<0.05	7.9	<0.1	7.2	
Element	Si	Fe	Mg	Ca	Al	As	B
(μg/L)	10,798	53	6066	966	102	613	3936

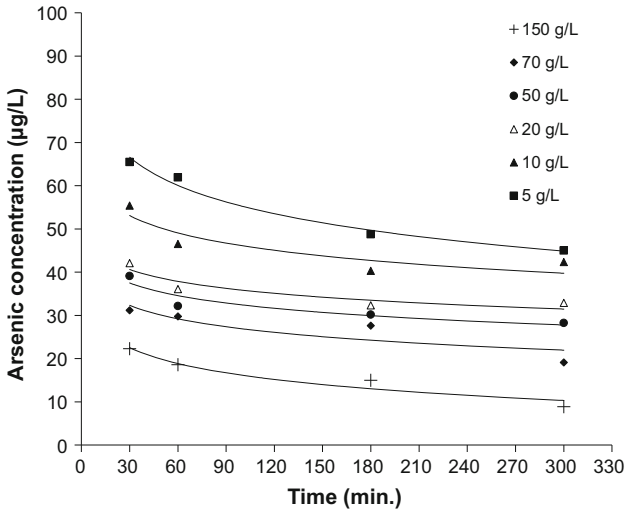

Fig. 6 Effect of dosage on the removal of arsenic from Emet-Hisarcık underground source water by PA (initial concentration: 613 μg/L; pH: 9; temperature: 25 °C)

OES (Mg, Ca, Si, Fe, Al, As, B). The results were analyzed, and F^-, NO_2^-, and PO_4^{3-} concentrations were less than 1 mg/L. The Cl^-, NO_3^-, and SO_4^{2-} concentrations ranged from 6.5 to 8 mg/L. The presence of Cl^- and NO_3^- does not significantly influence As removal (EPA 2000), nor does SO_4^{2-} at a pH of 9 to11. Although SO_4^{2-} decreases As removal at pH < 7 (Wickramasinghe et al. 2004), in this study, the initial pH was 9, and so the SO_4^{2-} concentration was not expected to be an issue.

In contrast, PO_4^{3-} can compete with As for adsorption sites (Guo et al. 2007; Meng et al. 2002). Guo et al. (2007) found that phosphate (at 10 mg/L) reduced As uptake by siderite from 54 to 28 % and by hematite from 69 to 36 %. However, the presence of dissolved PO_4^{3-} (at < 0.1 mg/L) did not affect As adsorption in this study.

The effect of silica on As adsorption depends on the silica concentration. Gebreyowhannes (2009) reported that As removal efficiency decreased by 25 % as the silica increased from 4.5 to 65 mg/L. Tuutijärvi et al. (2012) found that dissolved silica (at ≤ 10 mg/L) did not significant affect As removal. In this study, the competing effect of silicate (at ≤ 10 mg/L) was negligible (Table 6).

Arsenic Removal Tests

The As(V) removal increased with the amount of PA added over the range of 5–150 g/L. After a contact time of 300 min, the residual dissolved As concentration was 45 μg/L at a PA dosage of 5 g/L, compared with 8.87 μg/L at 150 g/L of PA (Fig. 6). The PA reduced the dissolved As concentration from an initial value of 600 to <10 μg/L. This is important since the groundwater in this region is used as drinking water (Çolak et al. 2003) and As exposure in the region leads to various skin diseases (Doğan and Doğan 2007).

Conclusions

The PA effectively removed As from borated water and the As adsorption was only weakly dependent on initial pH at ≤9. In fact, the addition of PA to water was found to have a buffering effect. Over an adsorption period of 5 h, the residual dissolved As was 6.8 μg/L at a pH of 9. The adsorption kinetics were well described by the pseudo-second-order model and the PA adsorption data fit the Langmuir isotherm equations well. The dimensionless separation factor (R_L) showed that PA was favored for the removal of dissolved As(V). The maximum adsorption capacity of the sorbent was 294 μg/g. The PA was able to remove up to 97 % of the As at an adsorbent dosage of 10 g/L, a solution pH of 9, a temperature of 25 °C, and an initial As concentration of 300 μg/L. Thus, PA can potentially be used as an effective, ready-to-use, and inexpensive adsorbent for As(V) removal from aqueous solutions.

Acknowledgments The authors thank the Karadeniz Technical University Scientific Research Fund (Project Kod No: 2013ARGEBD-9040) for the financial support of this work.

References

Aksoy N, Simsek C, Gunduz O (2009) Groundwater contamination mechanisms in a geothermal field: a case study of Balcova, Turkey. J Contam Hydrol 103:13–28

Alp I, Deveci H, Yazıcı EY, Türk T, Sungun H (2009) Potential use of pyrite cinders as raw material in cement production: results of industrial scale trial operations. J Hazard Mater 166:144–149

Altundoğan HS, Altundoğan S, Tümen F, Bildik M (2000) Arsenic removal from aqueous solutions by adsorption on red mud. Waste Manag 20:761–767

Arienzo M, Adamo P, Chiaenzelli J, Bianco MR, Martino A (2002) Retention of arsenic on hydrous ferric oxides generated by electrochemical peroxidation. Chemosphere 48:1009–1018

Aydın AO, Gulensoy H, Akıcıoğlu A, Sakarya A (2003) Effect of boric acid and borax production of arsenic in colemanite. J Sci Technol Inst 5:51–58

Balsamo M, Di Natale F, Erto A, Lancia A, Montagnaro F, Santoro L (2010) Arsenate removal from synthetic wastewater by adsorption onto fly ash. Desalination 263:58–63

Başkan BM, Pala A, Türkman A (2010) Arsenate removal by coagulation using iron salts and organic polymers. Ekoloji 19:69–76

Borah D, Senapati K (2006) Adsorption of Cd(II) from aqueous solution onto pyrite. Fuel 85:1929–1934

Bulut E, Özacar M, Şengil İA (2008) Equilibrium and kinetic data and process design for adsorption of Congo Red onto bentonite. J Hazard Mater 154:613–622

Chuang CL, Fan M, Xu M, Brown RC, Sung S, Saha B, Huang CP (2005) Adsorption of arsenic(V) by activated carbon prepared from oat hulls. Chemosphere 61:478–483

Clara M, Magalhães F (2002) Arsenic: an environmental problem limited by solubility. Pure Appl Chem 74:1843–1850

Colak M, Gemici U, Tarcan G (2003) The effects of colemanite deposits on the arsenic concentration of soil and groundwater in Igdekoy-Emet, Kutahya, Turkey. Water Air Soil Poll 149:127–143

Cong L (2004) Sorption/desorption of Arsenic to Nanometer Scale Magnetite. PhD Thesis, Rice Univ, Houston, TX

Dada AO, Olalekan AP, Olatunya AM, Dada O (2012) Langmuir, Freundlich, Temkin and Dubinin–Radushkevich isotherms studies of equilibrium sorption of $Zn2^{+}$ onto phosphoric acid modified rice husk. J Appl Chem 3:38–45

Doğan M, Doğan AU (2007) Arsenic mineralization, source, distribution, and abundance in the Kutahya region of the Western Anatolia, Turkey. Environ Geochem Health 29:119–129

Dubinin MM (1960) The potential theory of adsorption of gases and vapors for adsorbents with energetically nonuniform surface. Chem Rev 60:235–266

EPA (2000) Technologies and Costs for Removal of Arsenic from Drinking Water. Report 815-R-00-028, United States Environmental Protection Agency, Office of Water, Washington DC

Foo KY, Hameed BH (2010) Insights into the modeling of adsorption isotherm systems. Chem Eng J 156:2–10

Gebreyowhannes YB (2009) Effect of Silica and pH on Arsenic Removal by Iron-oxide Coated Sand. MSc Thesis Unesco-Ihe Institute for Water Education, Delft, the Netherlands

Genc H, Tjell JC, McConchie D, Schuiling O (2003) Adsorption of arsenic from water using neutralized red mud. J Colloid Interface Sci 264:327–334

Gimenez J, Martınez M, Pablo D, Rovira M, Duro L (2007) Arsenic sorption onto natural hematite, magnetite, and goethite. J Hazard Mater 141:575–580

Guo H, Stüben D, Berner Z (2007) Removal of arsenic from aqueous solution by natural siderite and hematite. Appl Geochem 22:1039–1051

Ho YS, McKay G (1998) Kinetic model for lead(II) sorption on to peat. Adsorp Sci Technol 16:243–255

Hobson JP (1969) Physical adsorption isotherms extending from ultra-high vacuum to vapor pressure. J Phys Chem 73:2720–2727

Huang HH, Lu MC, Chen JN (2001) Cataltic decomposition of hydrogen peroxide and 2-chlophenol with iron oxides. Water Res 35:2291–2299

Islam M, Mishra PC, Pate R (2011) Fluoride adsorption from aqueous solution by a hybrid thorium phosphate Composite. Chem Eng J 166:978–985

Jomova K, Jenisova Z, Feszterova M, Baros S, Liska J, Hudecova D, Rhodes CJ, Valko M (2011) Arsenic: toxicity, oxidative stress and human disease, review. J Appl Toxicol 31:95–107

Kroutil O, Chval Z, Skelton AA, Predota M (2015) Computer simulations of quartz (101)–water interface over a range of pH values. J Phys Chem 119:9274–9286

Kundu S, Gupta AK (2007) Adsorption characteristics of As (III) from aqueous solution on iron oxide coated cement (IOCC). J Hazard Mater 142:97–104

Lenoble V, Bouras O, Deluchat V, Serpaud B, Bollinger JC (2002) Arsenic adsorption onto pillared clays and iron oxides. J Colloid Interface Sci 255:52–58

Makris KC, Sarkar D, Datta R (2006) Evaluating a drinking-water waste by-product as a novel sorbent for arsenic. Chemosphere 64:730–741

Meng X, Korfiatis GP, Bang S, Bang KW (2002) Combined effects of anions on arsenic removal by iron hydroxides. Toxicol Lett 133:103–111

Mohan D, Pittman CU (2007) Arsenic removal from water/wastewater using adsorbents-a critical review. J Hazard Mater 142:1–53

Mondal P, Majumder CB, Mohanty B (2006) Laboratory based approaches for arsenic remediation from contaminated water: recent developments. J Hazard Mater 137:464–479

Mukherjee A, Sengupta MK, Amir Hossain MA, Ahamed S, Das B, Nayak B, Lodh D, Rahman MM, Chakraborti D (2006) Arsenic contamination in groundwater: a global perspective with emphasis on the Asian scenario. J Health Popul Nutr 24:142–163

Pecenyuk SI (1999) The use of the pH at the point of zero charge for characterizing the properties of oxide hydroxides. Russ Chem Bull 48:1017–1023

Raji C, Anirudhan TS (1998) Batch Cr(VI) removal by polyacrylamide-grafted sawdust: kinetics and thermodynamics. Water Res 32:3772–3780

Ravenscroft P, Brammer H, Richards K (2009) Arsenic pollution: a global synthesis. Wiley, Blackwell, London

Salim M, Munekage Y (2009) Removal of arsenic from aqueous solution using silica ceramic: adsorption kinetics and equilibrium studies. Int J Environ Res 3:13–22

Singh DB, Prasad G, Rupainwar DC (1996) Adsorption technique for the treatment of As(V)-rich effluents. Colloid Surf 111:49–56

Smedley PL, Nicolli HB, Macdonald DMJ, Barros AJ, Tullio JO (2002) Hydrogeochemistry of arsenic and other inorganic constituents in groundwaters from La Pampa, Argentina. Appl Geochem 17:259–284

Song S, Lopez-Valdivieso A, Hernandez-Campos DJ, Peng C, Monroy-Fernandez MG, Razo-Soto I (2006) Arsenic removal from high-arsenic water by enhanced coagulation with ferric ions and coarse calcite. Water Res 40:364–372

Tombacz E, Majzık A, Horvat ZS, Illes E (2006) Magnetite in aqueous medium: coating ıts surface and surface coated with it. Rom Rep Phys 58(3):281–286

Torrens KD (1999) Evaluating arsenic removal technologies. Pollut Eng 31:25–27

TS 266 (2005) Drinking water. Turkish Standards Institute, Ankara

Tugrul N, Derun EM, Piskin M (2007) Utilization of pyrite ash wastes by pelletization process. Powder Technol 176:72–76

Türk T, Alp I, Deveci H (2009) Adsorption of As(V) from water using Mg–Fe-based hydrotalcite (FeHT). J Hazard Mater 171:665–670

Türk T, Alp I, Deveci H (2010) Adsorption of As(V) from water using nanomagnetite. J Environ Eng 136:399–404

Tuutijärvi T, Repo E, Vahala R, Sillanpää M, Chen G (2012) Effect of competing anions on arsenate adsorption onto maghemite nanoparticles. Chin J Chem Eng 20:505–514

Vaughan RL, Reed BE (2005) Modeling As(V) removal by a iron oxide impregnated activated carbon using the surface complexation approach. Water Res 39:1005–1014

Veli S, Akyüz B (2007) Adsorption of copper and zinc from aqueous solutions by using natural clay. J Hazard Mater 149:226–233

WHO (1981) Arsenic, environmental health criteria 18 IPCS international program on chemical safety. Vammalankırjapaino, Vammala

WHO (1993) guidelines for drinking-water quality. Volume 1: recommendations, 2nd Edit, World Health Organization, Geneva, Switzerland

WHO (1996) Guidelines for drinking-water quality. Health criteria and other supporting information. Geneva, Switzerland, pp 940–949

Wickramasinghe SR, Han B, Zimbron J, Shen Z, Karim MN (2004) Arsenic removal by coagulation and filtration: comparison of groundwaters from the United States and Bangladesh. Desalination 169:231–244

Xu YH, Nakajima T, Ohki A (2002) Adsorption and removal of arsenic(V) from drinking water by aluminium loaded Shirazu-zeolite. J Hazard Mater 92:275–278

Zazouli MA, Balarak D, Mahdavi Y (2013) Application of *Azolla Filiculoides* biomass for 2-chlorophenol and 4-chrorophenol removal from aqueous solutions. Iran J Health Sci 1:43–55

Zhang W, Singh P, Paling E, Delides S (2004) Arsenic removal from contaminated water by natural iron ores. Miner Eng 17:517–524

Zhang S, Liu C, Luan Z, Peng X, Ren H, Wang J (2008) Arsenate removal from aqueous solutions using modified red mud. J Hazard Mater 152:486–492

Zhou YT, Nie HL, Branford-White C, He ZY, Zhu LM (2009) Removal of Cu^{2+} from aqueous solution by chitosan-coated magnetic nanoparticles modified with α-ketoglutaric acid. J Coll Interface Sci 330:29–37